PNAS
www.pnas.org

Supplementary Information for

Mangroves Protect Coastal Economic Activity from Hurricanes

Alejandro del Valle, Mathilda Eriksson, Oscar A. Ishizawa, and Juan Jose Miranda

Corresponding Alejandro del Valle or Mathilda Eriksson.
E-mail: adelvalle@gsu.edu or meriksson@gsu.edu

This PDF file includes:

www.pnas.org/cgi/doi/10.1073/pnas.1911617116

Supporting Information Text

SI1. Hurricane windstorm model. Hurricane wind speeds are calculated using the spatial hurricane windstorm model developed by the World Bank Group Latin America and the Caribbean Disaster Risk Management team (1). The model estimates maximum wind speeds at the height of 10 m with a spatial resolution of 1 km^2 for observed hurricanes and tropical storms in Central America during our sample period. The structure of this wind field model is based on the well-known equation for cyclostrophic wind and sustained wind velocity by (2) and is calibrated for the Central America region. The accuracy of the simulated wind speeds has been tested and validated with observed data. The estimated wind speeds (3) are only available for the following countries: Costa Rica, El Salvador, Honduras, Guatemala, Nicaragua, and Panama. The maximum sustained wind speed experienced in a particular location due to a hurricane is given by:

$$V = \frac{V_S \sin(\varphi) - f * r}{2} + \sqrt{\left(\frac{V_S \sin(\varphi) - f * r}{2}\right)^2 + \left(B \frac{\Delta p}{\rho}\right)\left(\frac{RMW}{r}\right)^B exp\left[-\left(\frac{RMW}{r}\right)^B\right]}$$

where B is the Holland shape parameter, Δp is the deficit of central and outer peripheral pressure (Pa), ρ is the air density at the gradient height (kg/m^3), RMW is the radius of maximum winds (m), r is the radius of any location to the center of the storm (m), V_S is the hurricane translation speed measured (m/s), f is the Coriolis parameter (1/sec), and φ is the angle between the north and the storm heading.

The data source for the terrain roughness is the Global Land Cover Dataset 2000, and for the topography is the Shuttle Radar Topography Mission database. The method to estimate speed-up occurring in escarpments and ridges comes from the American Society of Civil Engineers in 1994. The estimation method for wind gusts factors comes from (4). For more detailed information about the hurricane windstorm model and the data sources used see (1).

SI2. Implied monetary losses . To convert the benefit of mangrove protection (mitigation of hurricane damage), measured in nightlights, into rough monetary values, we begin by calculating a conversion factor between nightlights and economic activity as measured by Gross Domestic Product (GDP). Using World Bank data on GDP in Parity Purchasing Power (PPP) in constant 2011 international dollars, we derive average GDP and nightlights per km^2 for each country and year in our sample. Fig. S2 presents a scatter plot of GDP and average nightlights per km^2. The figure reveals a clear positive linear relationship between the two variables. To estimate this relationship, while accounting for changes in the measurement of nightlights, we regress GDP on nightlights and year fixed-effects. The estimated coefficient indicates that a one unit increase in nightlights per km^2 is associated with a \$225,838 increase in GDP per km^2 (p-value < 0.001).* Fig. S3 plots observed and predicted GDP using the product of nightlights and the estimated coefficient. Given that most observations are close to the 45-degree line, we conclude that this specification captures reasonably well the relationship between nightlights and GDP. To further verify the robustness of the previously estimated relationship, we use gridded GDP in constant 2011 international US dollars (5). Specifically, we combine this gridded GDP dataset, which provides information at the 5 arc-minute resolution (roughly 10 km^2 cells at the equator), with our nightlights dataset aggregated at the same resolution. We then regress GDP on nightlights and year fixed-effects. As before, we find a clear relationship between night lights and GDP. The estimated coefficient indicates that a one unit increase in nightlights is associated with a \$363,148 increase in GDP (p-value < 0.001).†

Next, we compute implied monetary losses in two steps. First, to derive observed total losses in terms of nightlights, we multiply each of the estimates from our preferred specification (Model 4 of Fig. 2) by the sum of the f damage index for each group. Second, we recover monetary losses by multiplying the previous results with our most conservative conversion factor of nightlights to GDP (\$225,838). To compute counterfactual hurricane losses in the absence of mangrove protection, we focus on the two groups where we find that mangroves mitigate the impact of hurricanes (1-2 km and 2 km or more of mangrove width). Specifically, we modify the first step by multiplying the sum of f for each of these two groups by the reduction in nightlights estimated for the group not protected by mangrove (less than 1 km of mangrove width). To account for uncertainty in our estimates of damages and the conversion factor between night lights and GDP we draw coefficients from a normal distribution with mean equal to the estimated coefficient and standard deviation equal to the standard error. This procedure is then repeated 5,000 times, using a random draw of the coefficients each time.

To illustrate the value of mangrove protection, we perform this calculation for coastal Nicaragua, which was affected by various hurricanes including the largest event in our sample, hurricane Felix. Fig. S4 plots the distribution of observed and counterfactual losses for each group with mangrove protection (1-2 km and 2 km or more of mangrove width). The counterfactual simulation suggests that average avoided monetary losses from mangroves are \$565,647 (std. dev. \$201,372) and \$403,769 (std. dev. \$143,743), respectively. Because the value of initially exposed economic activity protected by mangroves amounted to roughly \$39 million,‡ the estimates from the counterfactual simulation indicate that average combined avoided losses in this area (\$969,416) is roughly equivalent to 2.5%.

SI3. Distance placebo. We begin this exercise by performing an analogous calculation to that of Fig. 2 Model 2 (q = 3). The sample is the same as before but in this exercise we use the terciles of distance to the coast to construct the bins. Panel A Model 5 in Fig. S5 present the coefficients and 95% confidence intervals for this exercise. We find that, while noisily estimated,

*Standard errors are clustered at the country level. Because there are only 6 clusters, we also perform a wild cluster bootstrap (1000 iterations) procedure that yields a (p-value < 0.001).

†Standard errors are clustered at the 5-arc-minute cell level (6,135 clusters).

‡This can be calculated by summing nightlights in 2000 for this area and multiplying by the conversion factor.

the group that is closest to the coast (first tercile) experiences the largest reduction in nightlights, and that the impact of hurricanes progressively decreases with distance to the coast. Importantly, as shown in panel B, the groups that experience smaller reductions in nightlights (second and third tercile of distance) are also characterized by average mangrove widths of 0.99 and 1.36 km.

Next in panel A Model 6, we repeat the previous exercise excluding from the sample cells that have mangrove widths on their path to the coast longer than 1.5 km. As can be seen in panels B and C, this exercise allows us to construct bins that have a very similar distribution in terms of distance to the coast, but that have on average less than 0.6 km of mangrove width on their path to the coast. Turning to the results in panel A, while some coefficients are noisily estimated, we no longer find evidence of a decreasing pattern of hurricane impact. Panel A Models 7 and 8 repeat this placebo exercise, and find very similar results, when we exclude cells with 1.25 and 1 km of mangrove width on their path to the coast.

SI4. Robustness checks. We conduct several exercises to test the robustness of the model used to summarize the mangrove protection results. Specifically, we use Model 4 of Fig. 2 as our baseline specification. Column 1 of Table S1 provides standard errors under alternative assumptions for our baseline specification. These include robust standard errors clustered at the municipal level in parentheses (120 clusters); clustered at state level in brackets (35 clusters); and spatial heteroscedasticity and autocorrelation consistent errors in crochets (these errors, commonly referred to as Conley errors (6), are computed with 12 lags and a 500 km bandwidth). We find that in all cases the coefficient for the impact of hurricanes for the group with less than 1 km of mangrove width is statistically significant at conventional levels, and that the impact of hurricanes in areas protected by 1 km or more of mangroves remains statistically indistinguishable from zero. In column 2, we use the highest wind speed for every cell-year regardless of whether it is generated by the strongest hurricane in that year. We undertake this exercise to test whether important information has been discarded when we construct our cell-year panel using only information from the hurricane with the highest recorded wind speed. As can be seen, we recover nearly identical coefficients. Next, in columns 3 to 6, we use alternative assumptions to transform wind speed into potential damages. Specifically, column 3 uses a lower v_h parameter as suggested by (7); column 4 uses gale level winds to set a lower v_T parameter; and column 5 follows (8) and uses wind to the power of 8 instead of the f damage index. While the value of the reported coefficients changes because of the different transformations used, they consistently indicate similar levels of mangrove protection. To illustrate this point the row labeled "implied mangrove protection, cat 3" calculates the difference in damage (measured in nightlights) between cells with more and less than 1 km of mangrove width when they are affected by an upper range category three hurricane (208 km/h). The results indicate that for this type of hurricane, the losses averted by mangroves are between 0.96 and 1.66 nightlight units (our baseline estimate 1.2 nightlight units falls within this range). Next, in column 6, we restrict the sample to Guatemala, Honduras, and Nicaragua who experienced at least a category one hurricanes during our sample period. We find larger coefficients than those of our baseline specification, but a very similar estimate of mangrove protection 1.4 nightlight units. In column 7, we account for state-specific responses in the aftermath of hurricanes by introducing state-year fixed effects. We find similar coefficients of hurricane impact by level of mangrove protection. In column 8, we take advantage of the idea that coastline features are likely to be similar within small geographical areas, such as municipalities, and add municipal-year fixed effects. This specification allows us to account for confounding factors that are common to cells within a municipality in any given year. Because we find very similar estimates to those of column 1, we conclude that our results are not driven by coastline features that are common at the municipal level. Next in column 9, we show that our results are robust to relying on a lagged dependent variable specification by including 3 autoregressive lags instead of cell fixed effects. The number of lags was chosen by comparing the Akaike Information Criterion of models with different lags. We additional show in Fig. S6 that we can recover similar estimates when instead of binning mangrove width we instead include a multiplicative interaction with a quadratic polynomial, a cubic polynomial, or a logistic function of mangrove width. In all specifications we find that the impact of hurricanes on nightlights is fully mitigated in areas that are protected by approximately one km of mangrove width. Last, in column 10 of Table S1, we test whether our measure of mangrove width is robust to using a more stringent definition of the presence of mangrove. In the absence of a measure of mangrove density, we proxy density using the extent of forest cover. Specifically, we define a mangrove cell as dense if it has at least 50% forest cover in 2000 as reported in the (9) database. We then recompute our measure of mangrove width on the path to the coast and estimate Eq. 2. Because the bulk of our mangrove cell are found to be dense, we find nearly identical coefficient of the impact of hurricanes by level of mangrove protection.

SI5. Population protected by mangroves. To provide an illustration of the population that can be protected by mangroves, we use the CIESIN's GPW v4.11 downscaled population dataset (10). This dataset downscales input population counts at various scales to 30 arc-second cells (one km^2 at the equator) by assuming that population is uniformly distributed in space. Specifically, to obtain current population counts we use the UN WPP-Adjusted 2020 population projection raster. We begin by extracting for each cell in the raster the projected population count, we then merge the count to our main dataset and sum across cells that fall within our study area (storm surge prone areas). We then repeat this exercises for the subset of cells that have historically supported mangroves on their path to the coast, and for those cells protected by one km or more of mangrove on their path to the coast. Unlike in our main analysis, here we include in the dataset cells with zero nightlights during our sample period. The inclusion of this cells is necessary because our restricted sample would only include cells that are known to have a population (nightlights are observed) while the downscaled population data assumes that population is uniformly distributed (including cells without observed nightlights).

We find that almost 1.6 million people in our sample are highly exposed to hurricanes because they reside in storm surge prone areas. For this exposed population, we find that 0.8 million reside in cells that have historically supported mangroves on

their path to the coast, and can plausibly be protected through conservation or restoration efforts. We additionally find that roughly 0.3 million people are protected by one km or more of mangrove on their path.

While these population counts suggest that the benefits of mangrove protection extend to a substantial population, they should be interpreted with caution. As discussed in (11), a key limitation of the downscaled dataset is that population counts involving small geographical areas should be avoided when those areas are smaller than the input population data used to construct the (10). The input population data in Central America is generally coarse, as shown by our calculations from the Mean Administrative Unit Area raster of (10). The input population dataset in storm surge prone areas could be as large as 8,662 km^2 and was on average 2,168 km^2. Unfortunately, because cells with mangroves on their path to the coast are, by and large, non-contiguous areas, obtaining our population counts for these cells implied summing over areas that are much smaller than their input population areas. Accordingly, the counts should be interpreted as a rough measure of the exposed population which benefits from mangrove protection.

SI6. Replication.

SI6.1. Data availability. The data and code used in this paper can be found in the open ICPSR repository referenced in the paper.

SI6.2. Software. ESRI ArcGIS v10.4.3 was used for spatial data analysis and for the construction of the dataset. Stata v15 was used to perform all statistical analyses. Graphs were constructed using R v3.5.2.

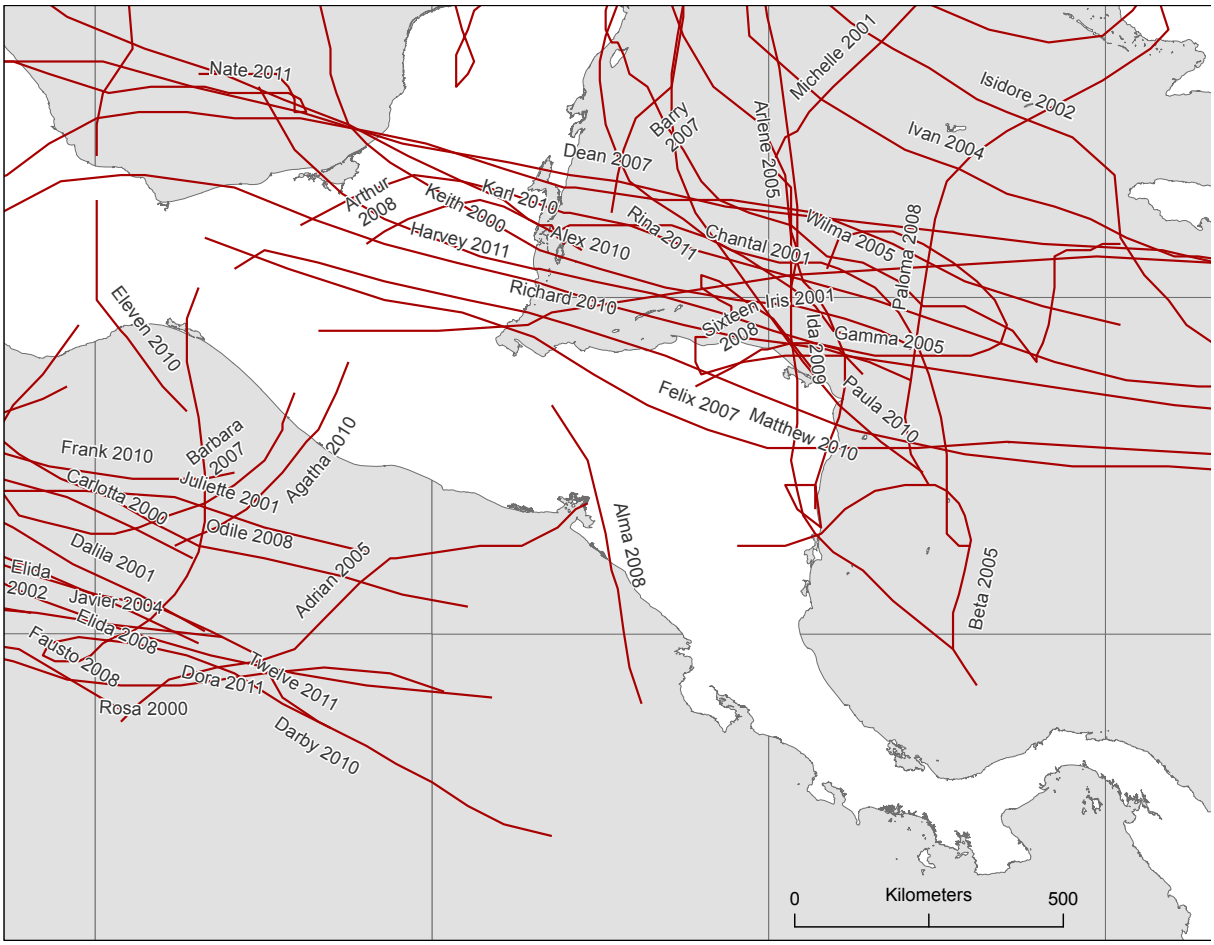

Fig. S1. Tracks of tropical storms and hurricanes.

This figure plots the tracks of tropical storms and hurricanes in our sample. Authors calculations based on HURDAT data.

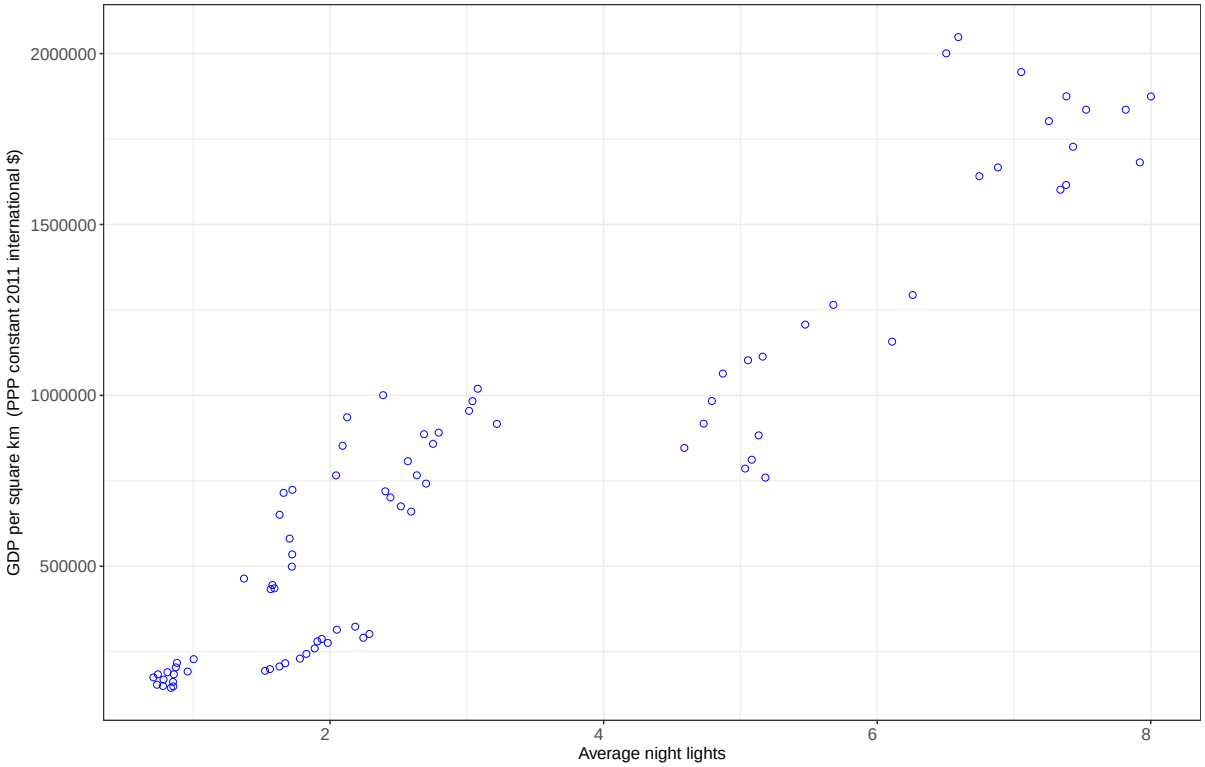

Fig. S2. GDP per km^2 and average nightlight intensity for each country and year

Scatter plot of the gross domestic product (PPP in 2011 international dollars) per km^2 and the average nightlight intensity per km^2 for each country and year (2000-2013).

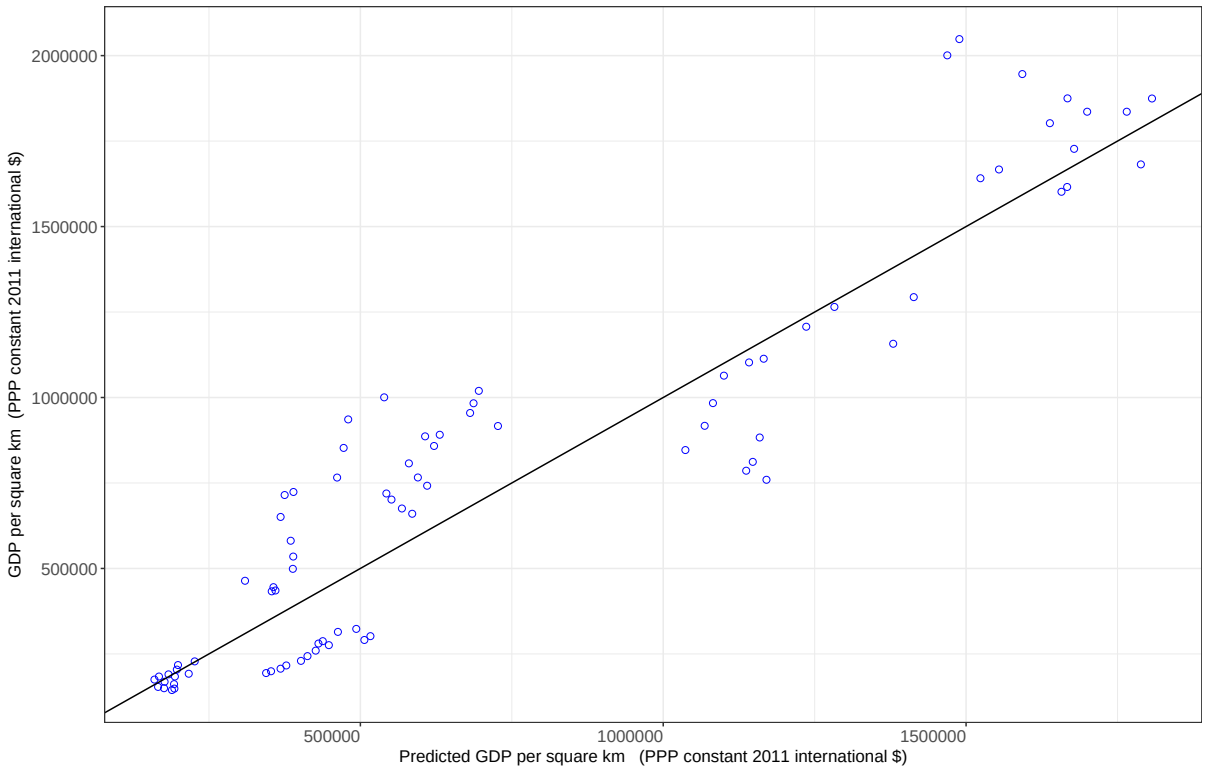

Fig. S3. Actual and predicted GDP per km^2 for each country and year

Scatter plot of the actual and estimated gross domestic product (PPP in 2011 international dollars) per km^2 for each country and year (2000-2013).

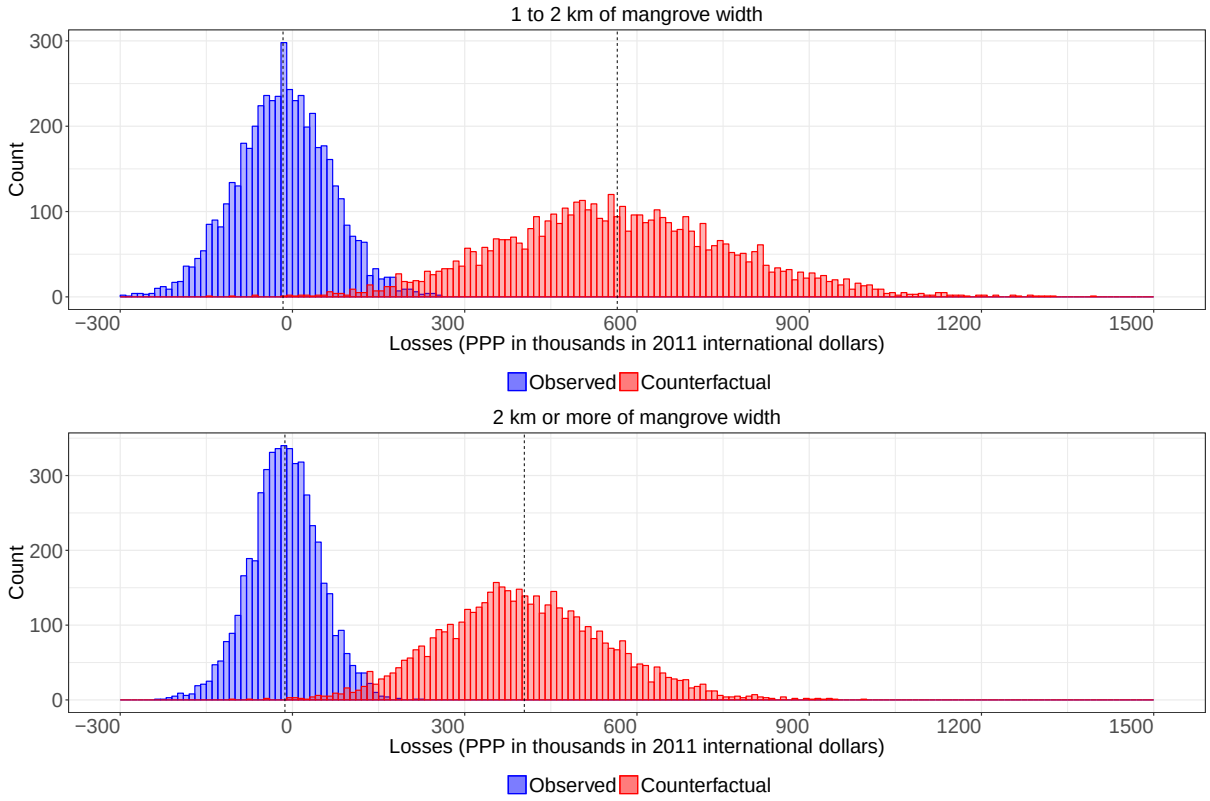

Fig. S4. Distribution of observed and counterfactual monetary losses.

This figure plots, for two groups currently protected by mangroves in coastal Nicaragua (1-2 km and 2 km or more of mangrove width), the distribution of implied monetary losses both observed and counterfactual (had mangrove been absent). Observed losses are calculated by multiplying the estimates for each bin from our preferred specification (Model 4 of Fig. 2) by the sum of the f damage index for each group. To express these losses in PPP 2011 international dollars, we then multiply the total losses in nightlight units previously derived by the nightlight to GDP conversion factor. To account for uncertainty in both our estimates of damages and the conversion factor between nightlights and GDP ($225,838), in each case we draw coefficients from a normal distribution with mean equal to the corresponding estimated coefficient and standard deviation equal to the standard error. This procedure is then repeated 5000 times, using a random draw of the coefficients each time. The resulting implied monetary losses are then plotted. The procedure to derive counterfactual losses is analogous, but we multiply the sum of f for each of these two groups by the reduction in nightlights estimated for the group not protected by mangrove (less than 1 km of mangrove width). The dashed lines represent the average for observed and counterfactual losses for each group.

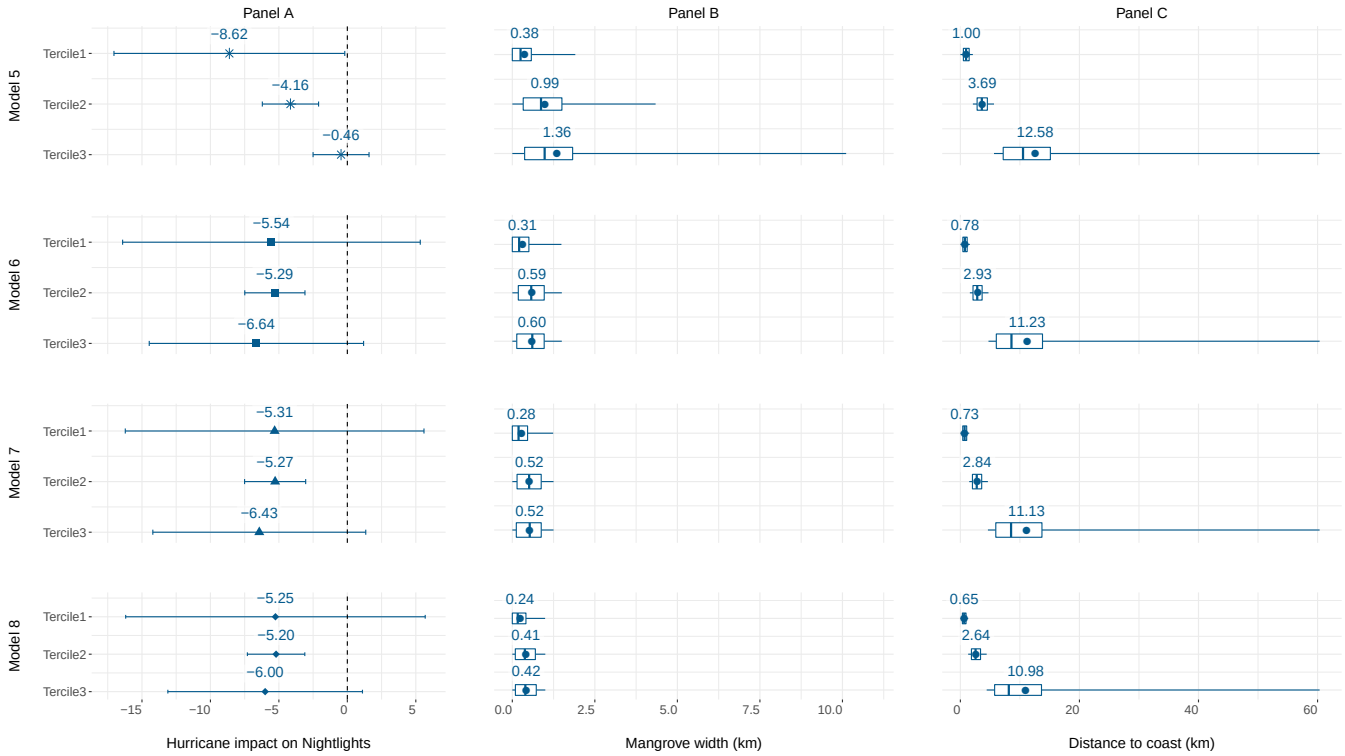

Fig. S5. Impact of hurricanes on nightlights by distance to coast

Panel A plots point estimates and 95% confidence intervals for four models. In Model 5 we discretize the distance to the coast variable into tercile bins and estimate the impact of hurricanes on economic activity for each bin. Models 6, 7 and 8, estimate Model 5 excluding from the sample cells that are protected by mangrove on their path to the coast: Model 6 excludes cells with more than 1.5 km; Model 7 exclude cells with more than 1.25 km; Model 8 excludes cells with more than 1 km. Panel B plots the distribution of mangrove width for each bin, and Panel C plots the distribution of distance to the coast for each bin. In panels B and C the box represents the interquartile range, the whiskers are the minimum and the maximum, and the dot is the average value.

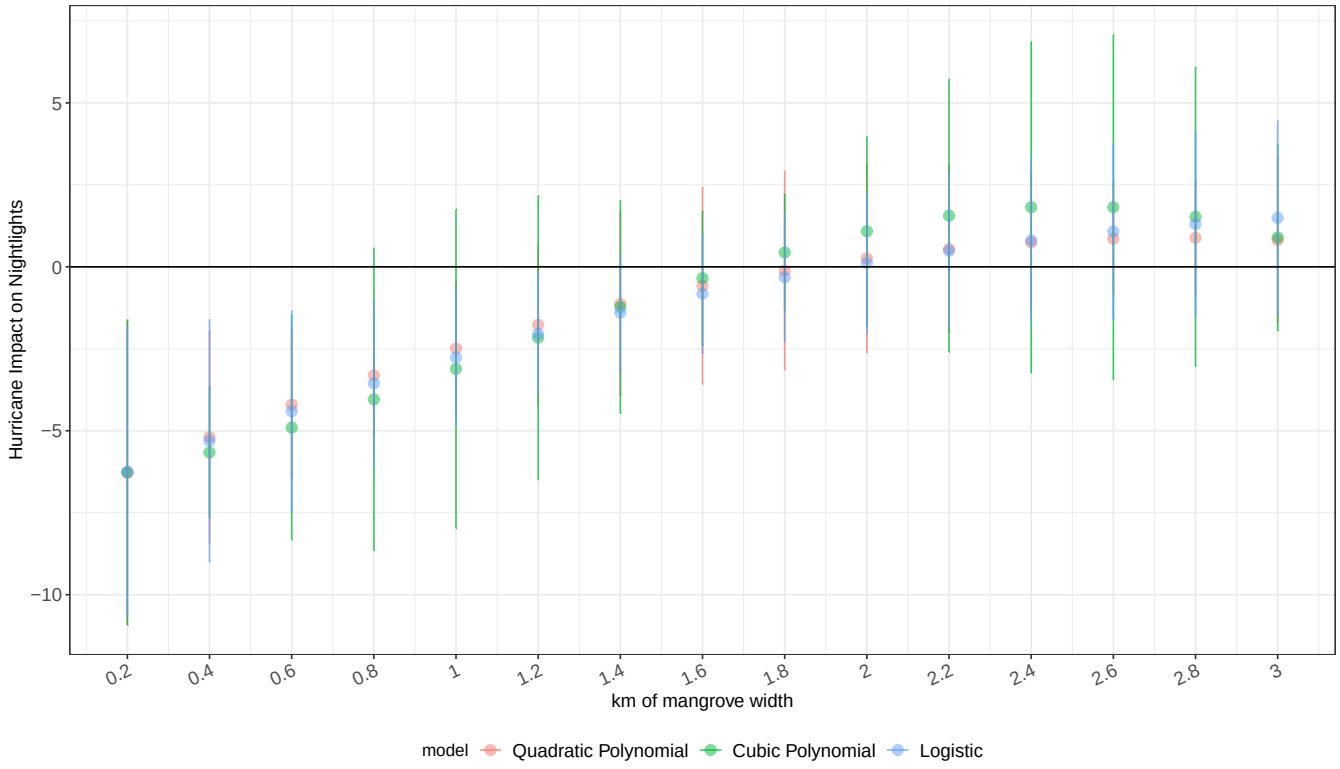

Fig. S6. Impact of hurricanes on nightlights by mangrove width

The figure plots point estimates and 95% confidence intervals for the marginal effects of three models. Specifically, each model is derived by estimating equation 2 after including an interaction between the f damage index and a quadratic polynomial, a cubic polynomial, or a logistic function of mangrove width. Marginal effects at 0.2 km intervals of mangrove width are then derived and plotted for each model.

Table S1. Robustness Mangrove Protection

	(1)	(2)	(3)	(4)	(5)	(6)	(7)	(8)	(9)	(10)
f 0-1 km mangrove width	-5.849	-5.378	-1.768	-4.619	-1.89×10^{-17}	-9.049	-6.487	-5.942	-7.768	-5.852
	(1.860) [2.307] {2.676}	(1.875)	(0.640)	(1.807)	(5.22×10^{-18})	(1.899)	(2.946)	(3.445)	(2.763)	(1.861)
f 1-2 km mangrove width	0.185	0.188	0.022	-0.231	5.04×10^{-19}	-1.964	-0.793	1.149	-0.625	0.166
	(0.842) [1.241] {1.975}	(0.842)	(0.277)	(0.883)	(2.91×10^{-18})	(0.825)	(2.419)	(0.963)	(1.034)	(0.842)
f >2 km mangrove width	0.195	0.198	0.029	0.363	1.55×10^{-18}	-2.042	-0.828	1.189	-0.328	0.254
	(0.879) [1.295] {2.105}	(0.879)	(0.291)	(0.830)	(2.91×10^{-18})	(0.863)	(2.507)	(0.997)	(1.082)	(0.857)
Observations	50,089	50,089	50,089	50,089	50,089	24,011	50,076	49,998	42,383	50,089
Implied mangrove protection, cat. 3	1.209	1.209	0.961	1.111	1.658	1.401	1.132	1.426	1.488	1.221
V threshold (km)	92.6	92.6	92.6	75.63	-	92.6	92.6	92.6	92.6	92.6
V half (km)	277.8	277.8	203.72	277.8	-	277.8	277.8	277.8	277.8	277.8

Dependent variable nightlights. Estimates from OLS regressions, cell and year fixed effects included but not reported. Mangrove protection is the difference in damage (measured in nightlights) between cells with more and less than 1 km of mangrove width when they are affected by a category three hurricane (208 km/h). Robust standard errors clustered at the municipal level in parentheses (120 clusters); clustered at state level in brackets (35 clusters); Conley errors in crochets (12 lags and a 500 km bandwidth). Column 2 uses the highest wind speed for every cell-year regardless of whether it is generated by the strongest storm in that year. Column 3 uses a lower v_h parameter as suggested by (7). Column 4 uses gale level winds to set a lower v_T parameter. Column 5 follows (8) and uses wind to the power of 8 instead of the f damage index. Column 6 restricts the sample to countries that experience at least a category one hurricanes during our sample period (Guatemala, Honduras, and Nicaragua). Column 7 includes state-year fixed effects. Column 8 includes municipal-year fixed effects. Column 9 includes 3 autoregressive lags. Column 10 uses only dense mangrove (at least 50% forest cover) to calculate mangrove width on the path to the coast.

References

1. GL Pita, R Gunasekera, O Ishizawa, Windstorm hazard model for disaster risk assessment in Central America. Proc. 14th Int. Conf. on Wind. Eng. Porto Alegre, Brazil (2015).
2. GJ Holland, An analytic model of the wind and pressure profiles in hurricanes. *Mon. Weather. Rev.* **108**, 1212–1218 (1980).
3. GL Pita, R Gunasekera, O Ishizawa, (2015) Data from: Windstorm hazard model for disaster risk assessment in Central America, Wind Speed Dataset. Available at: https://wbg.app.box.com/files/0/f/8796037069/Monthly_NTL_–_CA_and_Bolivia Accessed November 10, 2016.
4. PJ Vickery, PF Skerlj, Hurricane gust factors revisited. *J. Struct. Eng.* **131**, 825–832 (2005).
5. M Kummu, M Taka, JH Guillaume, (2019) Data from: Gridded global datasets for Gross Domestic Product and Human Development Index over 1990-2015, GDP_PPP_1990_2015_5arcmin dataset. Available at https://datadryad.org/stash/dataset/doi:10.5061/dryad.dk1j0. Accessed September 4, 2019.
6. TG Conley, GMM estimation with cross sectional dependence. *J. Econom.* **92**, 1–45 (1999).
7. K Emanuel, Global warming effects on us hurricane damage. *Weather. Clim. Soc.* **3**, 261–268 (2011).
8. WD Nordhaus, The economics of hurricanes in the United States (NBER Working Paper No. 12813) (2006) National Bureau of Economic Research, Cambridge, MA.
9. MC Hansen et al., (2014) Global Forest Change 2000-2014, 2000 percent tree cover dataset. Available at http://earthenginepartners.appspot.com/science-2013-global-forest. Accessed November 2, 2016.
10. Center for International Earth Science Information Network (CIESIN). Columbia University, (2017) Gridded Population of the World, Version 4.11, Population Count Adjusted to Match 2015 Revision of UN WPP Country Totals. Available at https://sedac.ciesin.columbia.edu/data/collection/gpw-v4. Accessed: September 9, 2019.
11. CIESIN, Documentation for the Gridded Population of the World, Version 4 (GPWv4), Revision 11 Data Sets. Palisades NY: NASA Socioeconomic Data and Applications Center (SEDAC). (2018).